Biomass Conversion and Biorefinery (2024) 14:21963–21978
https://doi.org/10.1007/s13399-023-04277-8

ORIGINAL ARTICLE

Overproduction of poly-β-hydroxybutyrate in *Methylosinus trichosporium* 11131 as degradable food packaging material utilizing methane

Noor Mohammed[1] · John Kiran Katari[2] · Debasish Das[1]

Received: 16 February 2023 / Revised: 31 March 2023 / Accepted: 25 April 2023 / Published online: 8 May 2023

Abstract

Biological conversion of methane into poly-β-hydroxybutyrate (PHB) presents a promising strategy for addressing greenhouse gas emissions and plastic pollution. This study presents a novel approach for the production of PHB from methane using *Methylosinus trichosporium* 11131. The integrated two-phase process involves the generation of high-density methanotrophic biomass in phase I, followed by the enrichment of PHB in phase II using nutritional modulation. Under optimal growth conditions, a biomass titer of 3.82 ± 0.01 g/L was achieved, and subsequent nitrate starvation led to the accumulation of PHB (41.24 ± 0.83 % w/w). Further optimization by exposing the cells to excess methane concentration (5% v/v) and nitrate starvation increased the PHB content to 52.42 ±1.03% w/w. The scalability of the process was demonstrated in a 5-L stirred tank bioreactor, yielding a PHB concentration of 2.02 ± 0.04 g/L. The suitability of the extracted PHB as a degradable food packaging material was evaluated by a comprehensive analysis of its thermal, structural, mechanical, physical, and molecular properties. Our results suggest that the PHB obtained from *Methylosinus trichosporium* 11131 can serve as a promising alternative to petroleum-based plastics due to its superior properties and biodegradability. Overall, this study presents an innovative biotechnological approach for the conversion of methane into a valuable biopolymer and highlights its potential as a sustainable alternative to conventional plastics.

Keywords Methanotroph · PHB · Methane · Degradable · Food packaging

Highlights
- Integrated two-phase process for biological conversion of methane into PHB.
- Phase I represents the generation of high-density (3.2 g/L) methanotrophic biomass.
- Phase II represents the enrichment of biopolymer (41.24% w/w) under nitrate starvation.
- Biopolymer content increased (52.42% w/w) under nitrate starvation and excess methane.
- Process was scaled up to a 5-L bioreactor with PHB titer of 2.02 g/L.
- Suitability of the biopolymer as degradable food packaging material was demonstrated.

Noor Mohammed and John Kiran Katari have contributed equally.

✉ Debasish Das
debasishd@iitg.ac.in; debasish.iitg@gmail.com

[1] Department of Biosciences & Bioengineering, Indian Institute of Technology, Guwahati, Assam 781039, India

[2] School of Energy Science and Engineering, Indian Institute of Technology, Guwahati, Assam 781039, India

1 Introduction

Amongst all the greenhouse gases (GHG), methane (CH4) is the second most detrimental, with the major sources being fossil fuels, power generation, agricultural waste, transportation, construction, land use and forestry, and anthropogenic activities [1]. Global methane emissions have increased by 162% to 570 million tons per year (Mt), with concentration rising to 1892.2 parts per billion (ppb). Plastic pollution, on the other hand, has become a critical environmental concern in the twenty-first century, currently with a global annual production of around 450 million tons [2]. Approximately, 40% of all consumer-used plastic is single-use and dumped each year whereas only 9–10% can be recycled. Globally, 22–43% of all plastic waste is disposed in landfills, while 50–80% of all litter into the ocean, posing a threat to the terrestrial and aqua-systems and, as a result, impacting human health [3].

To that end, the biological transformation of methane into value-added products can be a potential alternative over

conventional chemical conversion which requires extreme operating conditions [4]. Methanotrophs, a diverse group of Gram-negative bacteria, not only utilize methane for growth, but also produce poly-β-hydroxybutyrate, methanol, ectoine, single-cell protein, lipids, and extracellular polysaccharides [5]. Ray et al. (2023) highlighted the potential of methanotrophs to produce PHB and simultaneously address two critical global issues (i) mitigation of methane and (ii) synthesis of biodegradable biopolymer which can be a potential substitute to traditional plastics. PHB is an isotactic semi-crystalline biopolymer with water-resistant, high optical purity, piezoelectric capabilities, high tensile strength, high elasticity, heat tolerance, ease to mold, and can be blended with various co-polymers [6, 7]. Synthesis of PHB using methanotrophs occurs in two sequential steps: step 1, generation of high-density methanotrophic biomass using methane as carbon source, and step 2, enrichment of intracellular PHB. Type II methanotrophs are reported to accumulate a higher amount of intracellular PHB (up to 67%, w/w theoretically) on nutrient imbalance by effective utilization of the serine cycle [8, 9].

However, current technology to produce PHB from methane, using methanotrophs as a cell factory suffers disadvantages such as low mass transfer and low conversion efficiency, which ultimately result in lower biomass titer, PHB content, and PHB yield [10]. Recent studies reported improved PHB accumulation under modulation of macronutrients, e.g., nitrate and phosphate [8, 11–13] and micronutrients, e.g., copper (Cu), iron (Fe), magnesium (Mg), and potassium (K) [11, 13–18] present in the culture medium. Additionally, few simulation studies reported enhanced poly(3-hydroxybutyrate-co-3-hydroxyvalerate) production from methane using bubble column bioreactors [19, 20]. These studies provide important insights into the sustainable production of PHAs and offer simultaneous solution to address the problem of plastic pollution.

Methyosinus trichosporium 11131, a methanotroph, was used in the current study to develop a two-phase integrated process for the synthesis of PHB using methane as the only carbon source. In the first step, the production of high methanotrophic cell biomass (3.82 ± 0.01 g/L) was achieved under optimal media nutritional and process conditions. In the second stage, overproduction of PHB was attempted through the nutritional starvation of various macro- and microelements either individually or in combination, where maximum PHB content of 41.24 ±0.83% (w/w) was achieved under nitrate starvation. An overproduction of PHB at 52.42 ± 1.03% (w/w) was achieved by using this nutrient-depleted condition (nitrate starvation) in a combinatorial strategy with excessive carbon feeding (5% methane in air). Scale-up of the optimized process was performed in a 5-L continuous stirred tank bioreactor (CSTR), where a biomass titer of 3.94 ± 0.07 g/L and PHB content of 52.11 ± 0.31% (w/w) was observed. Further, a detailed characterization of extracted PHB was carried out and compared with low density polyethylene film (LDPE) properties to assess its potential application as an alternative packaging material for food, agriculture, pharmaceutical, and medical applications.

2 Materials and methods

2.1 Strain, culture conditions, and seed culture preparation

Type II methanotroph, *Methylosinus trichosporium* 11131 was procured from the National Collection of Industrial Food and Marine Bacteria (NCIMB, UK). It was cultured in nitrate mineral salt (NMS) media [21] containing macro-elements (g/L): KNO_3 (1.0), $CaCl_2$ (0.2), $MgSO_4.6H_2O$ (1.0), Fe-EDTA (0.0038), $Na_2MoO_4.2H_2O$ (0.00026), KH_2PO_4 (0.26), and $Na_2HPO_4.12H_2O$ (0.716). A trace metal solution (1 mL) containing microelements (g/L): $CuSO_4.5H_2O$ (0.2), $FeSO_4.7H_2O$ (0.5), $ZnSO_4.7H_2O$ (0.4), H_3BO_3 (0.015), $CoCl_2.6H_2O$ (0.05), EDTA disodium salt (0.25), $MnCl_2.4H_2O$ (0.02), and $NiCl_2.6H_2O$ (0.01) was added. All the media components were of analytical grade (HiMedia), and distilled water (18 MΩ) was used for media preparation. Seed culture was prepared in 500-mL air-tight customized bottles in NMS media with intermittent feeding of methane and air. Before autoclaving, the initial pH of the medium was adjusted to 6.8 using 1 M NaOH and 1 M H_2SO_4. The culture was kept under agitation at 150 rpm at 30 °C in an orbital shaking incubator (ORBITEK, Scigenics Biotech).

2.2 Characterization of *M. trichosporium* 11131 for PHB production

2.2.1 Evaluation of PHB accumulation under the influence of nutritional starvation

The culture of *M. trichosporium* 11131 for PHB production was performed under two phases: phase I (160 h duration) generation of high cell density methanotrophic biomass and phase II (32 h duration) enrichment of intracellular PHB in methanotrophic biomass produced in phase I. In phase I, high-density biomass was produced by CH_4 utilization using optimal process growth parameters maintaining methane concentration in the inlet gas stream at 2.5% v/v with air and a gas flow rate of 0.5 vvm [22]. Further, the initial concentration of nitrate, phosphate, and trace elements in the NMS media was kept at 610.16 part per million (ppm), 242.06 ppm, and, 0.75×, respectively [22]. Mid-log phase seed culture at an optical density (OD) of 5 at absorbance 600 nm was used as an inoculum for this phase (10% v/v).

In phase II, the methanotrophic biomass was subjected to complete nutritional starvation of individual macro and micro media components in NMS media such as (i) nitrate (KNO_3), (ii) phosphate ($Na_2HPO_4.12H_2O$ & KH_2PO_4), (iii) copper ($CuSO_4.5H_2O$), and (iv) iron ($FeSO_4.7H_2O$), and their combinations (i) nitrate and phosphate (N+P) and (ii) nitrate + copper (N + Cu) to assess its potential for PHB accumulation. The rest of the media components and operational conditions (2.5% methane with air) were kept similar in both phases. Methanotrophic biomass generated in phase I was harvested by centrifugation at 7000 rpm for 10 min. In phase II, an OD of 4 (1.68 g/L DCW) was set as the initial biomass concentration using phase I produced biomass. Both phases of operation were performed in a stirred-tank reactor of 1-L volume (800-mL working volume) containing a ring sparger of uniform pore size. The reactor was maintained at 30 °C under agitation using a water bath placed on a hot-plate magnetic stirrer (IKA C-MAG HS7).

2.2.2 Assessment of PHB production under the cumulative effect of nutritional starvation and carbon-excess condition

A process engineering strategy was designed to evaluate the combinatorial effect of nitrate starvation in NMS media (optimal parameters obtained from a nutritional starvation experiment), coupled with elevated methane concentration in the inlet gas stream on intracellular PHB accumulation. Here, no other nitrate source was taken except N_2 gas along with air. Three different concentrations of methane 2.5, 5.0, and 7.5% (v/v) with air in the gas inlet with 0.5 vvm flow rate were applied in combination with nitrate starvation conditions and intracellular PHB levels were estimated. Experiments were carried out in duplicate.

2.2.3 In situ esterification of methanotrophic biomass for quantitative estimation of PHB

Ten milligrams of vacuum-dried methanotrophic biomass was taken in a tightly sealed tube and 2 mL of dichloroethane was added followed by 2-mL propanol-containing HCl (4:1 v/v). The mixture was vortexed for 30 s and heated at 100 °C for 2 h in a shaking water bath. The sample was cooled down to room temperature and Milli-Q water (4 mL) was added and vortexed for 30 s. The lower organic phase containing PHB esters was quantified by gas chromatography [23].

2.2.4 Optimization of PHB extraction process from methanotrophic biomass

To enhance PHB extraction, three alternative solvent-based extraction methods—chloroform, chloroform: hypochlorite, and ethyl acetate (non-halogenated)—were chosen based on the solubility and toxicity of halogenated solvents [24]. Two hundred milligrams of methanotrophic biomass was vacuum dried using a Speedvac concentrator (Thermo Fisher Scientific), and the same was used for all the extraction methods. In the chloroform extraction method, 20 mL of chloroform was added to the biomass and incubated at 37 °C for 48 h under constant agitation at 100 rpm. The PHB was extracted by precipitation with 10 volumes of ice-cold methanol [25]. In the chloroform: hypochlorite method of extraction, 10 mL of chloroform and 10 mL of hypochlorite (10% v/v) were added to the biomass. The mixture was incubated for 1 h at 37 °C in a water bath and centrifuged at 5000 rpm for 5 min. PHB accumulated in the chloroform was separated. Following filtration, PHB was extracted by precipitation with ice-cold acetone and then dried at room temperature [24]. In the non-halogenated method of extraction, 20 mL of ethyl acetate was added to the biomass and was incubated at 25 °C for 1 h under 100 rpm agitation. After centrifugation at 5000 rpm for 10 min, the supernatant was separated and precipitated using ice-cold acetone and dried [24].

2.2.5 Batch cultivation in large-scale stirred tank bioreactor for growth and PHB production

M. trichosporium biomass was cultivated in both phases as phase I and phase II for scale-up production in a stirred tank bioreactor (New Brunswick TM Bioflo® 115, Eppendorf, Germany) with 5-L working volume for methanotrophic biomass and PHB production. In scale-up cultivation as phase I, optimized parameters: 2.5% CH_4 with air (20.48% oxygen) with flow rate of 0.5 vvm, nitrate (610.16 ppm), phosphate (242.06 ppm), and trace elements (0.75×) as obtained from earlier experiments (Section 2.1), with agitation 150 rpm at room temperature were used for high biomass density production, further to see the effect on PHB production on a scale-up. After 160 h, methanotrophic biomass was harvested with a centrifuge (ThermoFisher, Scientific, Heraeus Multifuge X3R) and re-suspended in phase II for PHB production under nitrate source starvation in NMS medium with 5 % (v/v) methane with air (19.95% oxygen) as same physical condition as for growth. Dynamic profiles for growth, pH, dissolved oxygen, and PHB production were obtained through regular sampling and analysis.

2.3 Casting of degradable thin film from PHB biopolymer

Two grams of PHB was dissolved in 50-mL chloroform and mixed using a magnetic stirrer (IKA C-MAG HS7). The mixture was sonicated at 40% amplitude with a pulse interval (5s ON/10s OFF) to remove the air bubbles from the solution. The solution was poured carefully onto a Teflon

plate and placed on a horizontal surface, and allowed to dry at room temperature for 24 h.

2.4 Characterization of PHB thin film produced from *M. trichosporium* 11131

Detailed characterization of methanotroph-produced PHB thin film was carried out to study the mechanical, structural, molecular, and thermal properties to determine its suitability as biodegradable food packaging material.

2.4.1 Thickness of the PHB thin film

The thickness of the PHB thin film was measured using a screw gauge (Mitutoyo 293-240-30) at various locations (center to periphery), and average values were reported.

2.4.2 Tensile strength and elongation break

Tensile strength and elongation break (ϵ_B %) were determined to study the mechanical properties of the PHB thin film. Rectangular thin film with dimensions (L × W × T: 10 cm × 7 mm × 0.1 mm) was analyzed using 5k N Universal Testing Machine (Zwick Roell, Model: Z005TN) with a load speed 1 mm min^{-1} procedure at room temperature.

2.4.3 Wettability assay

The hydrophobicity of the PHB thin film was determined by measuring the water contact angle on the surface of the film. A small drop (2 µL) of distilled water drop placed on PHB thin film, and static water contact angles were measured with standard goniometer FM140 (Krüss GmbH, Hamburg, Germany) equipped with a camera and analysis software (Drop Shape Analysis SW21; DSA1) at room temperature [26].

2.4.4 X-ray diffraction

PHB thin film was crushed using mortar-pestle, and powder form was analyzed on X-ray diffractometer (Rigaku Technologies, JAPAN, Model: Smart lab) with Ni filtered Cu Kα radiation (λ = 0.1541 nm) as X-ray source (40 kV, 40 mA) to produce the spectra at a scan rate of 3° min^{-1} in the 2θ ranges of 5–50° (Gupta et al., 2017).

2.4.5 Oxygen transfer rate

To estimate the oxygen transfer rate, a dry PHB thin film of 0.1 mm thickness was analyzed using the labthink gas permeability test system by differential-pressure method according to ISO 15105-1 standard (International standards) procedure. In the presence of pure oxygen (purity nearly 99.9%), the oxygen transmission rate was measured as the volumetric flow rate of O_2, unit $area^{-1}$, and $time^{-1}$ at 0.1 MPa pressure.

2.4.6 Water vapor transmission rate

Estimation of water vapor transmission rate (WVTR) was performed using Labthink Water vapor transmission rate test machine based on the standard test method for water vapor transmission of materials (ASTM E96, International standards). A dry PHB thin film of 0.1-mm thickness was analyzed at 90% relative humidity and 23±2 °C under atmospheric pressure. The steady water vapor flow in unit time, passing through the unit area was determined in terms of $g/m^2/h$.

2.4.7 Fourier transform infrared spectroscopy

PHB thin film was analyzed using an FTIR spectrometer (Model No.: IRAffinity-1; Make: M/s Shimadzu, Japan) under attenuated total reflection (ATR) mode at an ambient temperature according to Gupta et al. [27]. After 16 scans at wavenumbers ranging from 650 to 4000 cm^{-1}, the spectra were generated and analyzed.

2.4.8 Field emission scanning electron microscope

A field emission scanning electron microscope (Zeiss, Gemini 300) was used to analyze the surface topography of the thin PHB film at different magnifications (2Kx, 5Kx, 10Kx, 20Kx). Thin film samples were mounted onto black carbon tape. After 30 s of gold sputtering, images were captured (2–4 kV accelerating voltage) [27].

2.4.9 Gel permeation chromatography

Molecular weight and the polydispersity index of PHB thin film were determined with a gel permeation chromatography (GPC) instrument (Waters Corporation, USA; software: Empower-2) attached to a refractive index detector (Varian RI-2414). PHB sample was dissolved in tetrahydrofuran (THF) (5 mg/mL concentration), and 50 µL of the sample was injected and run at a flow rate of 0.75 mL/min with a run time of 15 min. Molecular weight was determined using polystyrene as a standard [28, 29].

2.4.10 Differential scanning calorimetry and thermal gravimetric analysis

The thermal stability of the biopolymer was measured using differential scanning calorimetry (DSC)/thermal gravimetric analysis (TGA) instrument (NETZSCH DSC 3500). The thermograph was recorded by heating 5 mg of the sample from 30 to 600 °C with a temperature ramping of 10 °C/min

[27]. Based on the analysis, melting temperature, crystallization temperature, rate of mass loss (%/min), and maximum degradation temperature were determined.

2.4.11 Degradability assay

A degradability assay was performed in 1 M NaOH buffer solution (500 mL) with an initial pH set of 7.8. Small pieces (5cm ×5cm) of PHB thin film were dipped into the buffer solution at 58±2 °C for a duration of 30 days. Variations of pH in buffer solution and weight loss were analyzed [30].

2.5 Analytical methods

To monitor cell growth, the absorbance of the culture was measured at 600 nm (A_{600}) using a UV-Vis spectrophotometer (Cary Series 100, Agilent Technologies). The absorbance values were converted into dry cell weight (DCW) using the correlation, one optical density = 0.42 g dry cells/L (R^2 = 0.99). pH was measured using a pH meter (Mettler Toledo, Switzerland). Analysis of PHB was performed by gas chromatography (GC7890B, Agilent), equipped with an HP-5 column and flame ionization detector (FID) after in situ esterification of methanotrophic biomass. One-microliter sample was injected through an auto-sampler with a split ratio of 1:50 with helium (He) as carrier gas at a flow rate of 0.7 mL/min. The initial temperature of the oven was set at 80 °C (holding time: 2 min), with ramping of 10 °C/min for a duration of 6 min. The FID temperature was set at 275°C for PHB detection [31]. Nitrate concentration in the media was estimated by the salicylic acid method [32], and phosphate concentration in the media was estimated based on the ascorbic acid method [33]. All the experiments were performed in duplicates. Statistical significance was calculated with one way ANNOVA using Minitab21 software at 95% ($\alpha = 0.05$) confidence level, and the yield of PHB extracted from methanotrophic biomass was estimated by the formula:

$$\text{PHB yield } (\%) = \left(\frac{\text{Weight of PHB}}{\text{Weight of biomass}}\right) \times 100 \quad (1)$$

3 Results and discussion

3.1 PHB induction in high-density methanotrophic biomass under naturally induced nutritional starvation

In phase I, to achieve high-density biomass of *M. trichosporium* 11131, the culture was grown under optimized media composition according to Sahoo et al. [22]. A maximum biomass concentration of 3.82 ± 0.01 g/L was achieved after 160 h of batch cultivation with a biomass productivity of 0.64 ± 0.01 g/L/days and a methane fixation rate of 0.39 ± 0.01 g/L/days. An increase in pH from 6.8 to 8 was observed during the growth phase. The results obtained were similar to those attained in the study by Sahoo et al. [22]. The nitrate and phosphate were almost consumed by the organism within 160 h as shown in Fig. 1a. A dynamic profile of intracellular PHB storage during the growth shows a 4–8% w/w PHB accumulation in lag and exponential phase as observed in Fig. 1a. Further, to study the natural ability of *M. trichosporium* to accumulate PHB after complete utilization of nitrates and phosphates in the media, phase I cultivation was allowed to continue for an extended period of 208 h. In situ estimation of PHB content in the biomass shows upregulation in the intracellular PHB content with a maximum value of 23.03 ± 0.89 % w/w on the 9th day (216 h) of cultivation, which was comparable to other reports [11, 34–37]. Various literature reported induction of the intracellular PHB accumulation as a result of nutrient depletion [12, 17, 38]. Further, a decrease in PHB level was observed till the end of the batch at 240 h. This study provided information on *M. trichosporium* 11131's potential to produce PHB under naturally induced starvation. This could be further enhanced by a combined strategy of high cell-density biomass production in phase I coupled with nutrient starvation in phase II [39]. So, based on the time at which complete nitrate was utilized, and maximum biomass titer was achieved, phase I was ended, and phase II was initiated in the subsequent experiments to assess PHB production under nutritional starvation.

3.1.1 Evaluation of PHB levels in phase I generated methanotrophic biomass under induced nutritional starvation in phase II

Under nutritional starvation, methanotrophs undergo stress conditions and accumulate PHB inside the cell [40]. The high-density methanotrophic biomass produced in phase was subjected to nutritional starvation in phase II to evaluate its effect on PHB accumulation. Since, PHB accumulation is not growth associated; this strategic combination of two phases serves as a feast and famine strategy to accelerate biomass growth with sufficient nutrition in phase I and induce carbon storage in the form of PHB in phase II [13, 29, 41, 42]. Also, this strategy could prevent the decrease in PHB production in subsequent batches, caused due to repeated starvation conditions [36]. In comparison with the single-stage cultivation in the control experiment (Fig. 1a), two phase cultivation (Fig 1b–d) resulted in a reduction of time required for PHB accumulation. In single-stage cultivation, maximum PHB content was observed at 216 h of operation, while in two-stage cultivation maximum PHB was observed at 192 h (160 h of phase

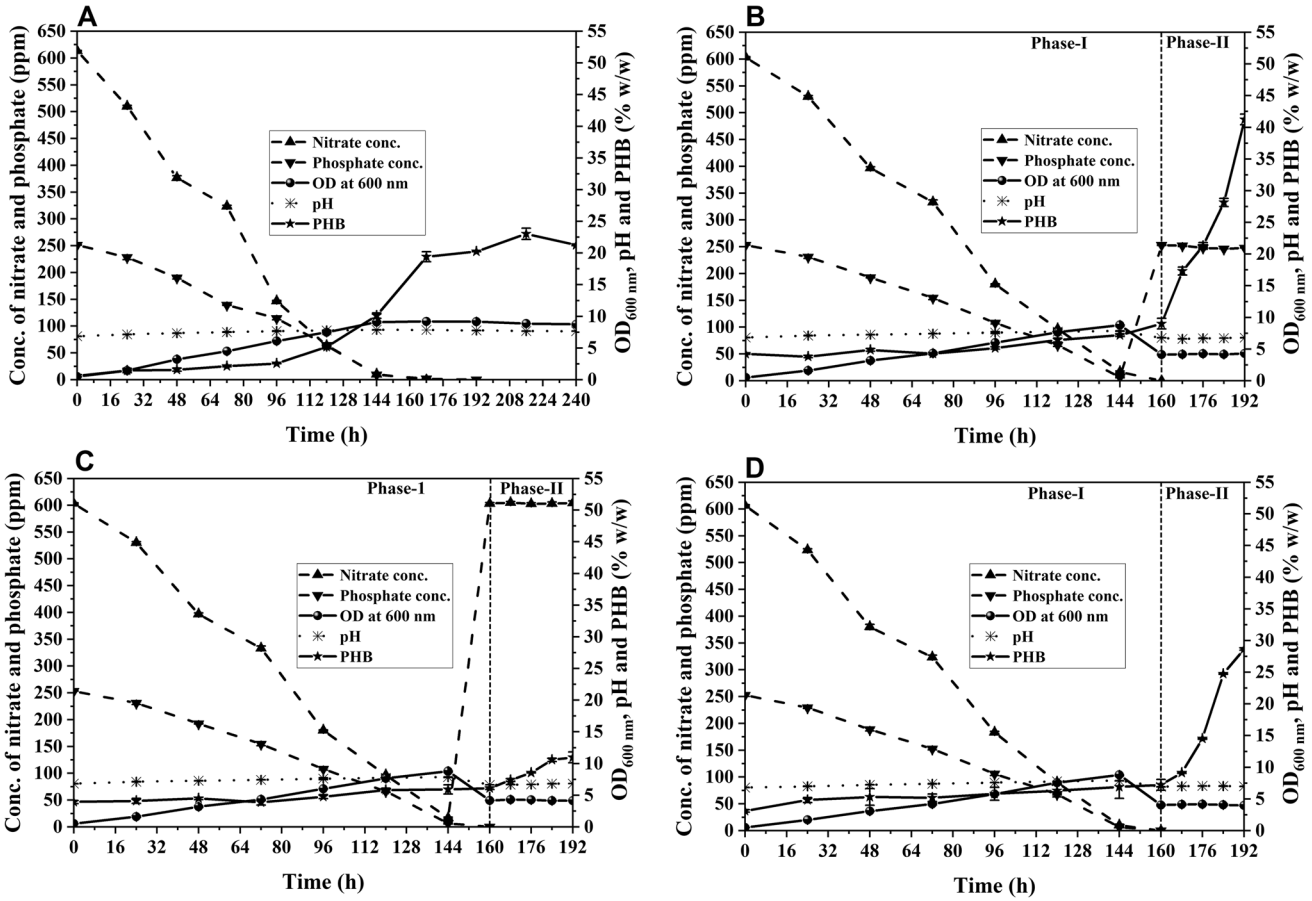

Fig. 1 Dynamic profile for growth, pH, nitrate, phosphate, and intracellular PHB content when *M. trichosporium* was cultivated under naturally induced nutritional starvation **a** single stage; and induced nutritional starvation in phase-I generated methanotrophic biomass under **b** nitrate, **c** phosphate, **d** combined nitrate and phosphate starvation in phase II for PHB induction. The significance level ($p \leq 0.05$) were obtained through statistical analysis using one way ANNOVA

I + 32 h of phase II). In the case of macro-element starvation (N, P, N+P), maximum carbon flux from methane is redirected towards intracellular PHB storage instead of growth. Under nitrate (N) source starvation, a PHB content of (41.24 ± 0.83% w/w) was observed after 32 h of phase II cultivation (Fig. 1b). This was attributed to the fact that under nitrogen-deficient conditions, the methanotrophic biomass shifted its metabolism towards PHB accumulation from the TCA cycle, thus resulting in high PHB accumulation [43].

This was in corroboration with other reports where a similar trend was observed concerning PHB accumulation under nutrient-deficient conditions [44–46]. The phosphate (P) starvation resulted in 10.97 ± 0.87 % w/w PHB content (Fig. 1c); while under combined nitrate and phosphate (N+P) source starvation, a PHB content of 28.66 ± 0.18% w/w was observed (Fig. 1d). This corroborated with other reported data where nitrate starvation resulted in PHB induction in the range of 29–50% [9, 13, 36, 47–51]. From the comparison of these three starvation conditions, it could be understood that nitrate starvation is most influential towards the accumulation of intracellular PHB.

Furthermore, the starvation of microelements such as Copper (Cu) and Iron (Fe) on PHB production was evaluated. As shown in (Fig. 2a and b), it was observed that on starvation of Cu and Fe, a PHB content of 13.04 ± 0.01% w/w and 6.49 ± 0.76% w/w was achieved, respectively. While Fe starvation did not induce much PHB accumulation, Cu starvation could only result in a comparably higher level. This could be attributed to their crucial role in methane monooxygenase enzyme activity (MMO) which is directly linked to methane assimilation [16, 34, 40, 52–54].

As Fe and Cu are required for normal activity of particulate MMO, their starvation might have caused a decrease in MMO activity and therefore resulted in lower levels of carbon transfer into PHB synthesis pathway [16, 55–57]. Further, under combined nutritional starvation of nitrates and Cu (N+Cu), a PHB content of 21.12 ± 0.42 % (w/w) was observed (Fig. 2c). This decrease in PHB content even under nitrate starvation might also

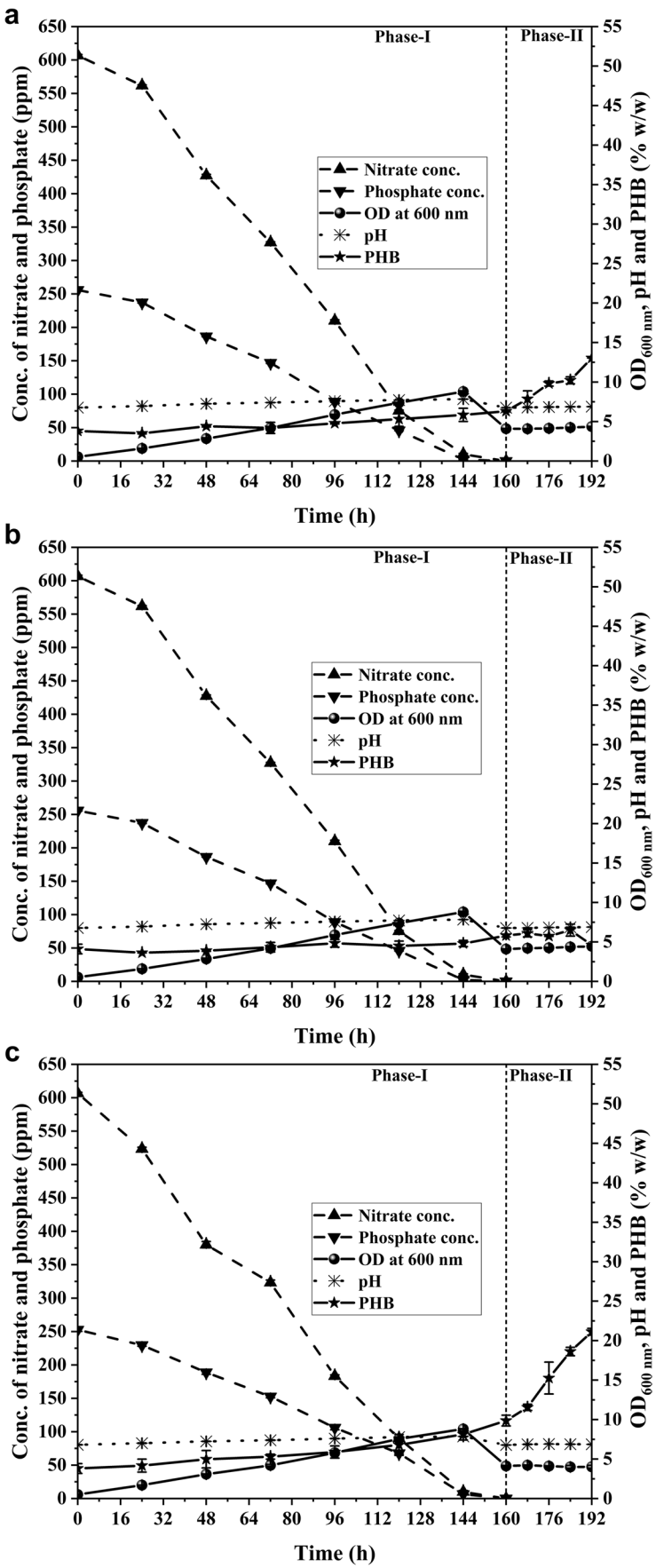

Fig. 2 Dynamic profile for growth, pH, nitrate, phosphate, and intracellular PHB content when phase-I generated *M. trichosporium* biomass was cultivated for phase II under induce nutritional starvation of **a** Cu, **b** Fe, and **c** combined nitrate + Cu. The significance level ($p \leq 0.05$) were obtained through statistical analysis using one way ANNOVA

be attributed to the absence of Cu required for normal activity of MMO. Therefore, it can be understood that the presence of Cu is very critical for PHB accumulation even under nitrate starvation conditions. Based on this, new strategies combining nitrate starvation with an excess of microelements (Cu or Fe) may be employed to enhance PHB content in methanotrophs.

3.2 Overproduction of PHB under the combinatorial influence of excess methane coupled with nutritional starvation

Removal of only nitrate resulted in the highest PHB content among all other nutritional starvation conditions. This nutrient-deficient condition was selected and further applied in a combinatorial strategy with excessive carbon feeding. The methane content in the gaseous mixture was elevated to 5.0 and 7.5% from 2.5%. Under the combination of 5% CH_4 (Fig. 3a) and nitrate starvation condition, excess carbon intake under nitrate starvation resulted in improved PHB accumulation. Maximum PHB content of 52.42 ± 1.03% (w/w) was observed under this condition after 32 h. While nitrate starvation conditions have resulted in shifting the metabolism to PHB storage, the simultaneous availability of excess methane resulted in greater availability of carbon source redirected into PHB synthesis. However, on further enhancement of methane percentage, a decrement in PHB storage was observed (46.64 ± 0.26% w/w) (Fig. 3b). This could be attributed to the inability of the microorganism to further utilize excess carbon. This result was in corroboration with reported literature where an intracellular PHB content of 17–48.7% (w/w) was achieved under induced nutritional starvation [9, 28, 37, 47, 50].

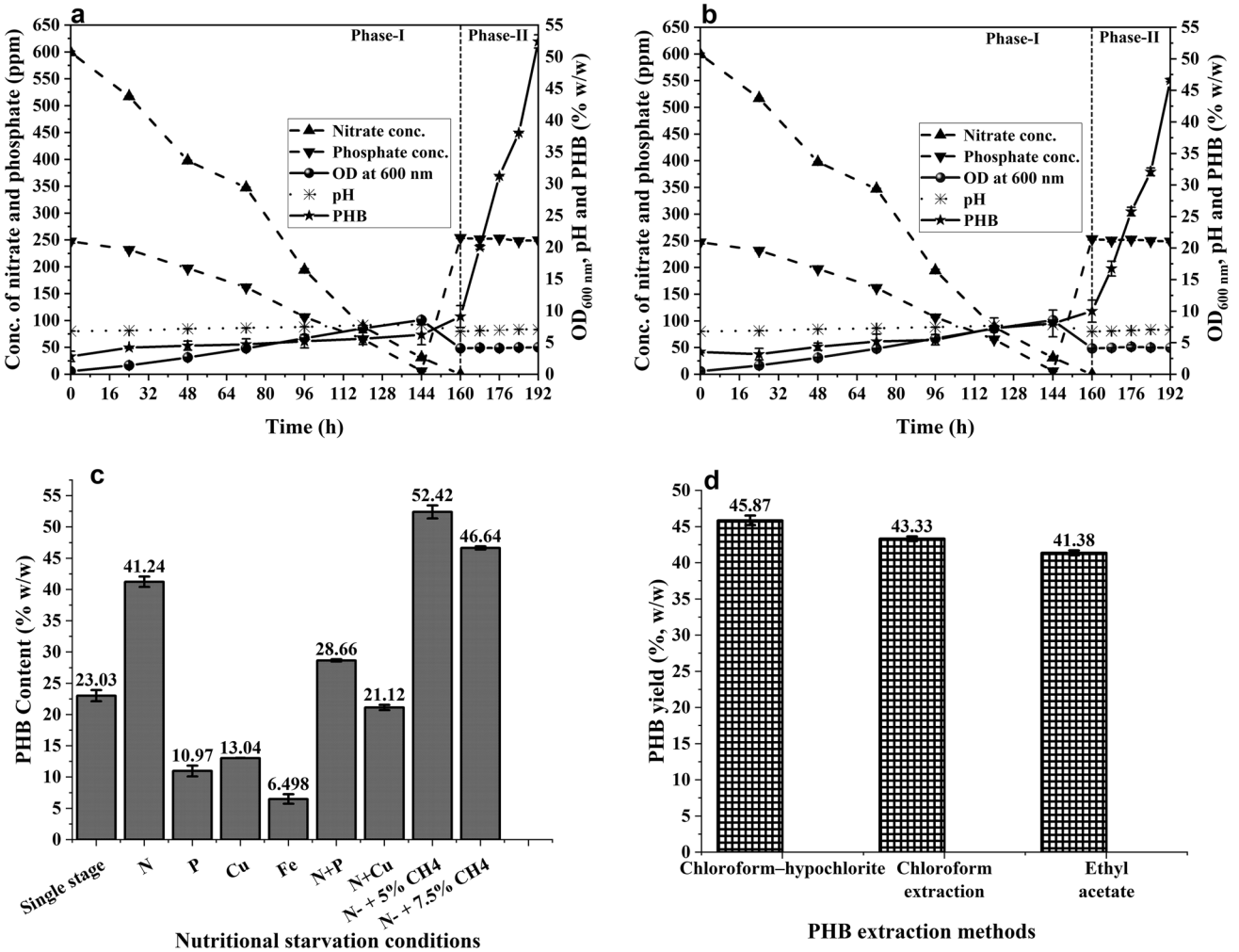

Fig. 3 Dynamic profile for growth, pH, nitrate, phosphate, and intracellular PHB content when *M. trichosporium* was cultivated under **a** combined nitrate starvation and 5% methane in the air; **b** combined nitrate starvation and 7.5% v/v methane in the air; **c** intracellular PHB content under different nutritional starvation conditions in phase II compared with naturally induced starvation in the single stage; **d** PHB yield in under different extraction methods. The significance level ($p \leq 0.05$) were obtained through statistical analysis using one way ANNOVA

3.3 Optimization of PHB extraction from *M. trichosporium* biomass

To extract maximum PHB from methanotrophic biomass, optimization of extraction methods viz. chloroform–hypochlorite dispersion extraction, chloroform extraction, and non-halogenated solvent (ethyl acetate) was performed. Maximum PHB yield was observed using chloroform–hypochlorite dispersion extraction at 45.87 ± 0.67% (w/w), followed by conventional chloroform extraction with a yield of 43.33 ± 0.33% and ethyl acetate extraction at 41.38 ± 0.33%. Considering the high yield level of the chloroform-hypochlorite method, this extraction method was used in all the experiments (Fig. 3d).

3.4 Scale-up of optimized process in a 5 L in continuous stirred tank bioreactor

Scale-up of the optimized bioprocess was demonstrated in a stir tank bioreactor (Fig. 4b) with continuous feeding of methane to achieve high biomass density and PHB yield. A maximum biomass titer of 3.94 ± 0.07 g/L was observed after 160 h of growth with a change in pH from 6.8 to 7.95 in phase-I as shown in (Fig. 4a).

During the growth of methanotrophs, a sharp decline in dissolved oxygen levels (87–4%) was observed during 16–24 h. Phase II cultivation with optimized parameters (nitrate source starvation + 5% v/v methane in the air) for overproduction of PHB resulted in maximum PHB content of 51.11 ± 1.03% (w/w) with a PHB titer of 2.02 ± 0.04 g/L after 32 h. It could be observed that dissolved oxygen sharply decreased with an increase in PHB content. A similar pattern of oxygen demand in methanotrophic cells has been reported during PHB production in other studies as well. In comparison with other studies under the batch mode, this work demonstrated an improved biomass titer and PHB content [11–13, 18, 35, 49], demonstrating the effectiveness of the optimized bioprocess and its potential for large-scale PHB production from methane.

3.5 Formation of degradable thin film from PHB biopolymer extracted from *M. trichosporium* and characterization of thin film

Figure 4c and d show PHB extracted from *M. trichosporium* 11131 chloroform-hypochlorite extraction method. Figure 4e shows the mixture of PHB dissolved in chloroform poured on the Teflon plate for casting. After 24 h of drying, a smooth film was formed as shown in (Fig. 4f). The thin film was further characterized to evaluate its potential as degradable packaging material.

3.5.1 Thickness

The average thickness measured by screw gauge of the PHB thin film, 0.1 ± 0.01 mm, makes it a suitable candidate for food packaging applications; in addition, the film's thickness can be adjusted to meet specific packaging requirements for different types of food product. Another study also has reported the application of 0.1-mm-thick film for edible food packaging [58].

3.5.2 Fourier transform infrared spectroscopy

The FTIR analysis provides important information on the molecular structure and bonding of PHB, which is useful for designing and optimizing its properties for degradable food packaging applications. FTIR spectrum of polyhydroxy-3-butyrate extracted from *M. trichosporium* is shown in (Fig. 5a). The peaks at 826 and 976 cm^{-1} represent C-C bond stretching of PHB in amorphous and crystalline phases respectively [59], while peaks at 1051 and 1098 cm^{-1} represent asymmetric stretching of first and second C-O (right-most) saturated aliphatic ester O-C-C bond respectively. Peak bands 1129 and 1181 cm^{-1} represent symmetric and asymmetric C-O-C bond stretching of aliphatic ester in the amorphous form of PHB. Peaks at 1224 and 1273 cm^{-1} represent symmetric C-O stretching of aliphatic ester in crystalline PHB. The band at 1379 represents the C-H symmetric stretching of methyl and 1453 cm^{-1} represents the asymmetric bending of methyl or methylene group in PHB polymer. The prominent and characteristic peak at 1722 represents the symmetric stretching carbonyl group (C=O) of the ester bond in crystalline PHB. While absorption bands obtained at 2934 and 2976 cm^{-1} represent alkane (–CH) bonding asymmetric and symmetric in the methyl group and minor divergence at 3,442 cm^{-1} corresponds to a terminal –OH group [60, 61]. In addition, PHB extracted from *M. trichosporium* was observed to be similar in chemical structure to PHB extracted from other microbes *B. megaterium* and *C. necator* [62].

3.5.3 Gel permeation chromatography

GPC analysis of PHB film indicates 2 peaks and a major peak at 5.925 min with an Mn value of 1.42×10^5, Mw value of 2.1×10^5 Da, and polydispersity index of 1.47. In general, the molecular weight of PHB lies in the range of $1.7–2.4 \times 10^5$ Da literature as reported by Karthikeyan et al., 2015. Other studies also suggest that extracted PHB from *M. trichosporium* has a high molecular weight of 2.1×10^5 Da due to potassium (K) limitation along with nitrate source (KNO_3) starvation medium [16]. Furthermore, the high molecular weight and low PDI of PHB will result in an improved mechanical strength and stiffness of the film, making it more durable and resistant to tearing. These properties make this PHB a promising candidate for food packaging applications.

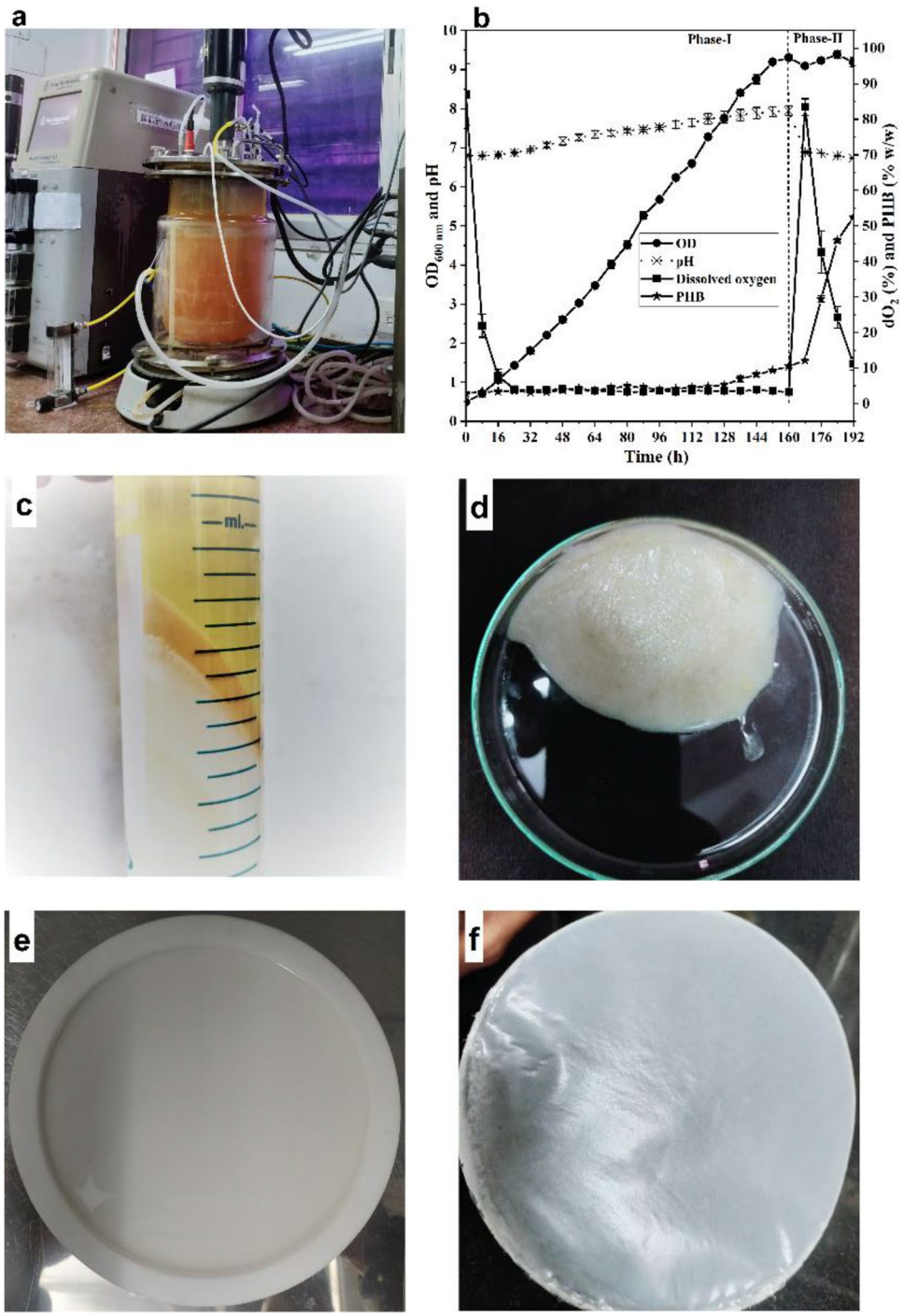

Fig. 4 **a** scale-up in 5-L stir tank reactor; **b** Dynamic profile for growth, pH, dissolved oxygen, and intracellular PHB content at the scale-up level under optimized process conditions (nitrate source starvation + 5% v/v methane in the air); **c** extraction of PHB from *M. trichosporium* biomass by chloroform–hypochlorite method; **d** extracted PHB; **e** casting of PHB thin film in Teflon-plate and; **f** PHB thin film (0.1 ± 0.01 mm). The significance level ($p \leq 0.05$) were obtained through statistical analysis using one way ANNOVA

3.5.4 Surface analysis

FESEM images at different magnifications 2K, 5K, 10K, and 20K were taken to analyze the surface morphology of thin PHB film as shown in (Fig. 5b-e). On higher magnification 2 µm pores were observed in conventional casting and molding of thin PHB film that could allow for the diffusion of gases and moisture, making it a potential degradable material for breathable food packaging, which can have significant environmental impacts.

3.5.5 X-ray diffraction analysis for the structural feature of PHB thin film

X-ray diffraction spectra of PHB thin film were analyzed as shown in (Fig. 6a). Peaks with miller indices were observed at 2θ = 13.4° (020), 16.8° (110), 21.4° (101), 22.5° (111), 25.4° (121), and 27.1° (040) representing the high degree of crystalline structure. The most intensive and scattered peaks at 2θ = 13.4° and 2θ at 16.8° confirm an orthorhombic unit cell which

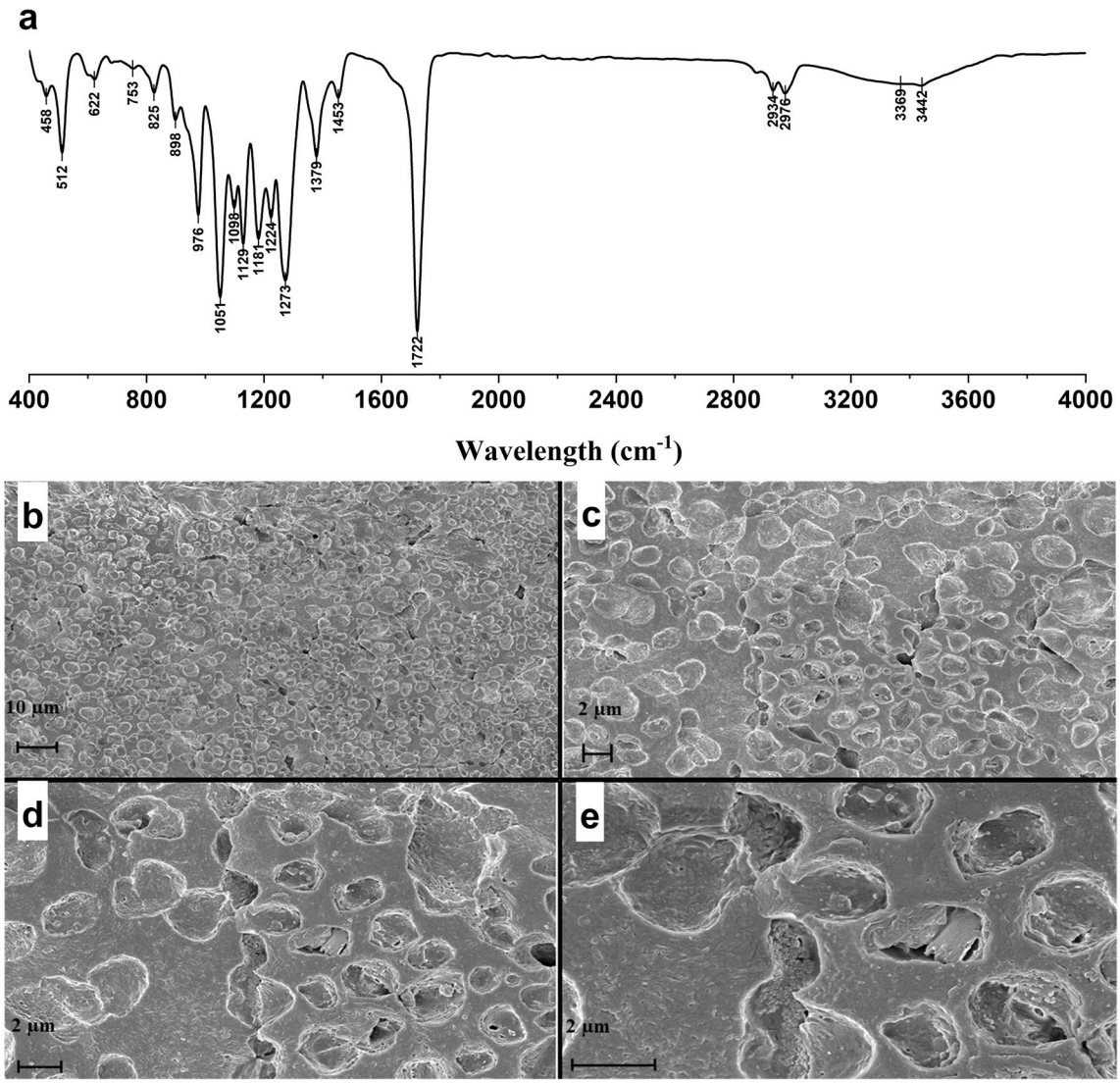

Fig. 5 Characterization of *M. trichosporium* 11131 extracted PHB thin film. **a** Fourier transform infrared spectroscopy (FTIR) spectrum; and FESEM images of PHB thin film under different magnifications. **b** 2Kx; **c** 5Kx; **d** 10Kx; and **e** 20Kx

was observed in other reports as well [62, 63]. Minor peaks at 2θ at 21.4° (101) and (111) and 2θ at 22.5°, represents α-form, while 2θ at 25.4° and 2θ at 27.1° indicate semi-crystalline nature. Further, the size of the PHB crystal was calculated to be 26.19 nm, with repeating unit cell lengths $a = 18.12$ Å, $b = 7.04$ Å, and $c = 10.23$ Å. *M. trichosporium*-produced PHB thin film possesses a high degree of crystallinity (76.6±2.6%) indicative of the mechanical and thermal strength of the polymer concerning as a packaging material.

3.5.6 Wettability assay

To qualify PHB material as food packaging material, it needs to be water resistant as it could come into contact with food materials. It is also required to ensure that the products are dry throughout handling, storage, and transportation. Therefore, the surface hydrophobicity was estimated based on water contact angle measurement. A surface having a water contact angle of water droplet $\theta > 68°$ is considered completely hydrophobic [35]. The average water contact angle on a thin film of PHB extracted from *M. trichosporium* 11131, was found to be 73.68° (Fig. 6b). These results from the contact angle measurement confirmed the hydrophobic nature of PHB film and supported its potential in degradable food packaging applications.

3.5.7 Mechanical strength analysis of PHB thin film

Mechanical characteristics mainly related to elasticity and tensile strength are to be assessed to determine the PHB material's strength under the application of physical forces

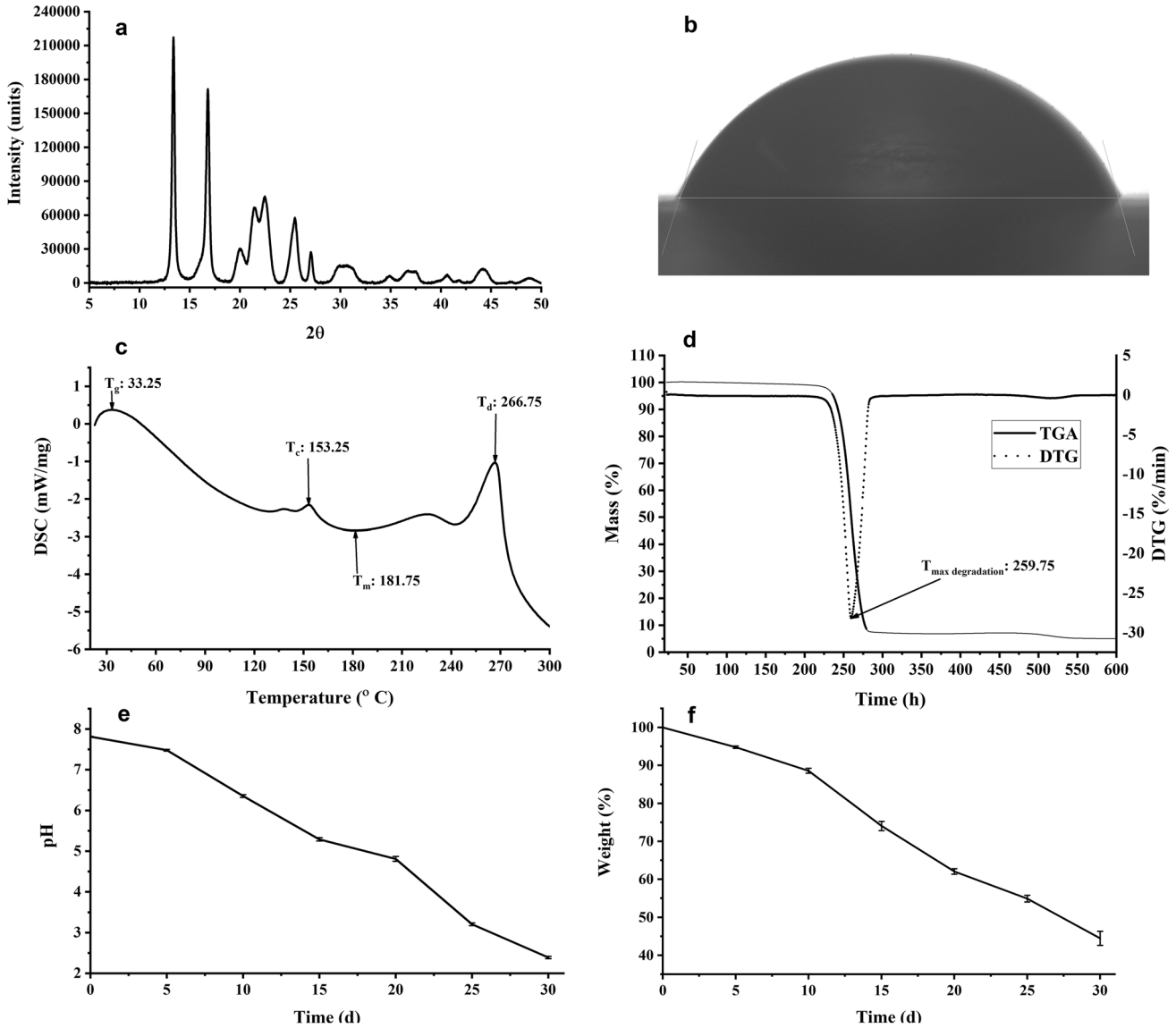

Fig. 6 Characterization of *M. trichosporium* 11131 extracted PHB thin film. **a** X-ray diffraction; **b** water contact angle; **c** DSC curve; **d** differential thermo-gravimetric analysis (DTG) and rate of mass (%) loss of PHB thin film; **e** and **f** variation in weight loss and pH during degradation. The significance level ($p \leq 0.05$) were obtained through statistical analysis using one way ANNOVA

is intended to be applied as packaging material. Analysis revealed a maximum tensile strength of 15.41 ± 0.34 MPa along with an elongation break (ϵ_B %) of 2.46 ± 0.19 and Young's modulus of 0.87 MPa. The results obtained proved its suitability as a packaging material with preferable mechanical properties.

3.5.8 Thermal analysis by DSC, TGA, and DTG

Thermal stability of green PHB polymer extracted from *M. trichosporium* by DSC (Fig. 6c) revealed a glass transition temperature of 33.25 °C, along with a crystallization temperature of 153.25 °C, melting temperature of 181.75 °C, and degradation temperature of 266.75°C. Thermal gravimetric (DTG) analysis (Fig. 6d) revealed maximum degradation of 60.23% with a weight loss rate of −28.19 % per minute observed at a maximum degradation temperature of 259.75°C [62, 64] confirming its thermal resistance.

3.5.9 Water vapor transmission rate

WVTR is critical to determine the weight gain of the PHB film caused due to moisture retention under constant pressure and temperature in 24 h of time (g.m^2/day). It was calculated using combined Henry-Fick's Law using equation WVTR ($\left(\mathrm{g/m^2}\right) \times 24\ \mathrm{h} = \frac{w}{A}$)), where *w* represents the weight (g) gain

Table 1 Comparison of *M. trichosporium* 11131 extracted PHB film properties with LDPE film

Properties	LDPE film	PHB film from the current study (0.1 ± 0.01 mm thickness)	References*
Tensile strength (MPa)	8.27–31.7*	15.41	[67]
Glass transition temperature (°C)	−25–10*	33.25	[67]
Crystallization temperature (°C)	95.44*	153.25	[68]
Melting temperature (°C)	98–115*	181.75	[67]
Degradation temperature	260–325*	266.75	[69]
Water contact angle (°)	≥ 65*	73.7	[26]
Oxygen transmission rate ($cm^3mm/m^2/day$)	7000–8000*	2198.92	[70]
WVTR ($g/m^2/day$)	15–25*	34.2	[70]
Degree of crystallinity (%)	50–65%*	76.6	[70]
Mol. weight ($\times 10^5$ Da)	1.5–1.65*	2.1	[71, 72]

of the film due to moisture-retention, in a duration of 24 h and *A* is the surface area (m^2) of the PHB thin film. WVTR of thin PHB film was measured in accordance with the ASTM E-96 method, and it was estimated to be 34.22 $g/m^2/day$. Based on the WVTR calculated, the methanotroph extracted PHB thin film qualifies to be applied for food packaging applications as well as degradable food packaging material [65].

3.5.10 Oxygen transmission rate

To determine the quality of PHB film under the influence of reactive oxygen gas in the atmosphere, oxygen transmission rate (OTR) testing was performed according to ISO: 15105-1 method. OTR estimation is important in determining the shelf life of packaging material and for the methanotrophic PHB thin film, it was estimated to be 2198.92 $cm^3/m^2/day$ at 0.1 MPa pressure. This higher value might be attributed to increased porosity in PHB thin film (as shown in FESEM images in (Fig. 5c–f) making it more permeable towards oxygen [26, 66].

3.5.11 Degradability assay

Degradability being the primary prerequisite quality for packaging material, PHB thin film from *M. trichosporium* was subjected to degradability testing as shown in (Fig. 6e–f). After every 5 days, the weight and pH were measured. A decrease in weight (55.54 %) was observed along with a reduction in pH from 7.8 to 2.3 indicative of the film getting degraded under the influence of the buffer.

3.6 Comparison of methanotrophic PHB film properties with low-density polyethylene

Post-characterization of methanotroph-produced PHB thin film, was compared to that of low-density poly ethylene (LDPE) properties to showcase its potential as an alternative degradable food packaging material (Table 1). The methanotrophic PHB film has shown comparable tensile strength with that of standard LDPE film. With respect to thermal properties, the PHB film showed superior glass transition and melting temperature values compared to that of LDPE film. This will be advantageous, as food packaging requires higher thermal stability values.

Also, in the case of the water contact angle, a higher degree of hydrophobicity was observed as compared to LDPE film. However, WVTR values obtained in this study are on the higher side, which indicates high moisture retention compared to LDPE. This could be due to the traditional way of classical molding and casting of the PHB thin film rather than fabrication using an extruder machine. In the case of the classical method, the film produced has a higher degree of pores, as a result causing increased moisture retention. In comparison with LDPE film, the low OTR value of PHB film is advantageous as it is indicative of the longer shelf life of the packaging material. While the methanotrophic biomass extracted PHB thin film showed its potential as a degradable food packing material, further improvements such as co-polymerization would make it a suitable degradable food packaging material and a sustainable alternative to conventional polymers.

4 Conclusion

The work demonstrated the critical role of nutrient elements (macro and micro) on PHB accumulation in methanotrophic cells of M. *trichosporium* 11131. Nitrate starvation resulted in significantly high levels of PHB accumulation, while micro-element starvation (Fe and Cu) resulted in low levels. The combinatorial influence of excess C-source (5% methane in the air) and nitrate starvation, methanotrophic biomass showed high PHB accumulation, confirming this as a promising strategy for improved PHB production. Further, based

on its thermal, mechanical, physical, and molecular properties, it can be confirmed that methanotrophic PHB thin film can serve as a potential degradable food packaging material.

Acknowledgements Noor Mohammed and John Kiran Katari are grateful to Ministry of Education, Government of India for their research fellowship.

Author contribution Noor Mohammed: planning and execution of experiments, analysis and interpretation of data, and manuscript preparation; John Kiran Katari: experimental design and manuscript preparation; Debasish Das: overall design, conceptualization, and supervision of the work and manuscript writing.

Data availability The datasets generated during and/or analyzed during the current study are available from the corresponding author on reasonable request.

Declarations

Ethical approval Not applicable.

Competing interest The authors declare no competing interests.

References

1. Fekete H, Kuramochi T, Roelfsema M et al (2021) A review of successful climate change mitigation policies in major emitting economies and the potential of global replication. Renew Sustain Energy Rev 137. https://doi.org/10.1016/j.rser.2020.110602
2. Bergmann M, Almroth BC et al (2022) A global plastic treaty must cap production. Science 376(6592):469–470. https://doi.org/10.1126/science.abq0082
3. Landrigan PJ, Stegeman JJ, Fleming LE et al (2020) Human health and ocean pollution. Ann Glob Heal 86:1–64. https://doi.org/10.5334/aogh.2831
4. Hwang IY, Nguyen AD, Nguyen TT et al (2018) Biological conversion of methane to chemicals and fuels: technical challenges and issues. Appl Microbiol Biotechnol 102:3071–3080. https://doi.org/10.1007/s00253-018-8842-7
5. Strong PJ, Xie S, Clarke WP (2015) Methane as a resource: can the methanotrophs add value? Environ Sci Technol 49:4001–4018. https://doi.org/10.1021/es504242n
6. Levett I, Birkett G, Davies N et al (2016) Techno-economic assessment of poly-3-hydroxybutyrate (PHB) production from methane - the case for thermophilic bioprocessing. J Environ Chem Eng 4:3724–3733. https://doi.org/10.1016/j.jece.2016.07.033
7. Xu J, Guo BH, Yang R et al (2002) In situ FTIR study on melting and crystallization of polyhydroxyalkanoates. Polymer (Guildf) 43:6893–6899. https://doi.org/10.1016/S0032-3861(02)00615-8
8. Asenjo JA, Suk JS (1986) Microbial conversion of methane into poly-β-hydroxybutyrate (PHB): growth and intracellular product accumulation in a type II methanotroph. J Ferment Technol 64:271–278. https://doi.org/10.1016/0385-6380(86)90118-4
9. Nguyen TT, Lee EY (2021) Methane-based biosynthesis of 4-hydroxybutyrate and P(3-hydroxybutyrate-co-4-hydroxybutyrate) using engineered Methylosinus trichosporium OB3b. Bioresour Technol 335:125263. https://doi.org/10.1016/j.biortech.2021.125263
10. Liu LY, Xie GJ, Xing DF et al (2020) Biological conversion of methane to polyhydroxyalkanoates: current advances, challenges, and perspectives. Environ Sci Ecotechnol 2:100029
11. García-Pérez T, López JC, Passos F et al (2018) Simultaneous methane abatement and PHB production by Methylocystis hirsuta in a novel gas-recycling bubble column bioreactor. Chem Eng J 334:691–697. https://doi.org/10.1016/j.cej.2017.10.106
12. Khosravi-Darani K, Mokhtari ZB, Amai T, Tanaka K (2013) Microbial production of poly(hydroxybutyrate) from C1 carbon sources. Appl Microbiol Biotechnol 97:1407–1424. https://doi.org/10.1007/s00253-012-4649-0
13. Wendlandt K, Jechorek M, Helm J, Stottmeister U (2001) Producing poly-3-hydroxybutyrate with a high molecular mass from methane. J Biotechnol 86:127–133
14. Doronina NV, Ezhov VA, Trotsenko IA (2008) Growth of Methylosinus trichosporium OB3b on methane and poly-beta-hydroxybutyrate biosynthesis. Prikl Biokhim Mikrobiol 44:202–206. https://doi.org/10.1134/s0003683808020099
15. Ghoddosi F, Golzar H, Yazdian F et al (2019) Effect of carbon sources for PHB production in bubble column bioreactor: emphasis on improvement of methane uptake. J Environ Chem Eng 7:102978. https://doi.org/10.1016/j.jece.2019.102978
16. Helm J, Wendlandt KD, Jechorek M, Stottmeister U (2008) Potassium deficiency results in accumulation of ultra-high molecular weight poly-β-hydroxybutyrate in a methane-utilizing mixed culture. J Appl Microbiol 105:1054–1061. https://doi.org/10.1111/j.1365-2672.2008.03831.x
17. Rostkowski KH, Criddle CS, Lepech MD (2012) Cradle-to-gate life cycle assessment for a cradle-to-cradle cycle: biogas-to-bioplastic (and back). Environ Sci Technol 46(18):9822
18. Wendlandt KD, Geyer W, Mirschel G, Al-Haj Hemidi F (2005) Possibilities for controlling a PHB accumulation process using various analytical methods. J Biotechnol 117:119–129. https://doi.org/10.1016/j.jbiotec.2005.01.007
19. Amabile C, Abate T, De Crescenzo C et al (2022) Sustainable process for the production of poly(3-hydroxybutyrate- co-3-hydroxyvalerate) from renewable resources: a simulation study. ACS Sustain Chem Eng 10:14230–14239. https://doi.org/10.1021/acssuschemeng.2c04111
20. Amabile C, Abate T, De Crescenzo C et al (2022) Poly(3-hydroxybutyrate) production from methane in bubble column bioreactors: process simulation and design optimization. N Biotechnol 70:39–48. https://doi.org/10.1016/j.nbt.2022.04.004
21. Patel SKS, Jeong JH, Mehariya S et al (2016) Production of methanol from methane by encapsulated Methylosinus sporium. J Microbiol Biotechnol 26:2098–2105. https://doi.org/10.4014/jmb.1608.08053
22. Sahoo KK, Datta S, Goswami G, Das D (2022) Two-stage integrated process for bio-methanol production coupled with methane and carbon dioxide sequestration: kinetic modelling and experimental validation. J Environ Manag 301:113927. https://doi.org/10.1016/j.jenvman.2021.113927
23. Riis V, Mai W (1988) Gas chromatographic determination of poly-β-hydroxybutyric acid in microbial biomass after hydrochloric acid propanoysis. J Chromatogr A 445:285–289. https://doi.org/10.1016/S0021-9673(01)84535-0
24. Aramvash A, Gholami-Banadkuki N, Moazzeni-Zavareh F, Hajizadeh-Turchi S (2015) An environmentally friendly and efficient method for extraction of PHB biopolymer with non-halogenated solvents. J Microbiol Biotechnol 25:1936–1943. https://doi.org/10.4014/jmb.1505.05053
25. Hahn SK, Chang YK, Lee SY (1995) Recovery and characterization of poly(3-hydroxybutyric acid) synthesized in Alcaligenes eutrophus and recombinant Escherichia coli. Appl Environ Microbiol 61:34–39. https://doi.org/10.1128/aem.61.1.34-39.1995

26. Arrieta MP, López J, Hernández A, Rayón E (2014) Ternary PLA-PHB-Limonene blends intended for biodegradable food packaging applications. Eur Polym J 50:255–270. https://doi.org/10.1016/j.eurpolymj.2013.11.009
27. Gupta A, Prasad A, Mulchandani N et al (2017) Multifunctional nanohydroxyapatite-promoted toughened high-molecular-weight stereocomplex poly(lactic acid)-based bionanocomposite for both 3D-printed orthopedic implants and high-temperature engineering applications. ACS Omega 2:4039–4052. https://doi.org/10.1021/acsomega.7b00915
28. Myung J, Flanagan JCA, Waymouth RM, Criddle CS (2017) Expanding the range of polyhydroxyalkanoates synthesized by methanotrophic bacteria through the utilization of omega-hydroxyalkanoate co-substrates. AMB Express 7. https://doi.org/10.1186/s13568-017-0417-y
29. Liu LY, Xie GJ, Xing DF et al (2020) Biological conversion of methane to polyhydroxyalkanoates: Current advances, challenges, and perspectives. Environ Sci Ecotechnology 2:100029. https://doi.org/10.1016/J.ESE.2020.100029
30. Kalita NK, Damare NA, Hazarika D et al (2021) Biodegradation and characterization study of compostable PLA bioplastic containing algae biomass as potential degradation accelerator. Environ Challenges 3:100067. https://doi.org/10.1016/j.envc.2021.100067
31. Juengert J, Bresan S, Jendrossek D (2018) Determination of polyhydroxybutyrate (PHB) content in Ralstonia eutropha using gas chromatography and nile red staining. Bio-Protocol 8:1–15. https://doi.org/10.21769/bioprotoc.2748
32. Cataldo DA, Maroon M, Schrader LE, Youngs VL (1975) Communications in soil science and plant analysis rapid colorimetric determination of nitrate in plant tissue by nitration of salicylic acid. Comm Soil Sci Plant Anal 6(1):71–80
33. Sinha A, Goswami G, Kumar R, Das D (2021) A microalgal biorefinery approach for bioactive molecules , biofuel , and biofertilizer using a novel carbon dioxide - tolerant strain Tetradesmus obliquus CT02. Biomass Convers Bioref. https://doi.org/10.1007/s13399-021-02098-1
34. Xin JY, Zhang YX, Zhang S et al (2007) Methanol production from CO2 by resting cells of the methanotrophic bacterium Methylosinus trichosporium IMV 3011. J Basic Microbiol 47:426–435. https://doi.org/10.1002/jobm.200710313
35. Karthikeyan OP, Chidambarampadmavathy K, Cirés S, Heimann K (2015) Review of sustainable methane mitigation and biopolymer production. Crit Rev Environ Sci Technol 45:1579–1610. https://doi.org/10.1080/10643389.2014.966422
36. Pieja AJ, Rostkowski KH, Criddle CS (2011) Distribution and selection of poly-3-hydroxybutyrate production capacity in methanotrophic proteobacteria. Microb Ecol 62:564–573. https://doi.org/10.1007/s00248-011-9873-0
37. Criddle CS, Billington SL, Frank CW (2014) Renewable bioplastics and biocomposites from biogas methane and waste-derived feedstock: development of enabling technology, life cycle assessment, and analysis of costs. https://www2.calrecycle.ca.gov/Publications/Download/1106?opt=dln. Accessed Aug 2014
38. Dedysh SN, Derakshani M (2001) Detection and enumeration of methanotrophs in acidic Sphagnum peat by 16S rRNA fluorescence in situ hybridization, including the use of newly developed oligonucleotide probes for Methylocella palustris. Appl Environ Microbiol 67:4850–4857. https://doi.org/10.1128/AEM.67.10.4850
39. Chu KH, Alvarez-Cohen L (1998) Effect of nitrogen source on growth and trichloroethylene degradation by methane-oxidizing bacteria. Appl Environ Microbiol 64:3451–3457. https://doi.org/10.1128/AEM.64.9.3451-3457.1998
40. Zhang T, Zhou J, Wang X, Zhang Y (2017) Coupled effects of methane monooxygenase and nitrogen source on growth and poly-β-hydroxybutyrate (PHB) production of Methylosinus trichosporium OB3b. J Environ Sci (China) 52:49–57. https://doi.org/10.1016/J.JES.2016.03.001
41. Dias JML, Lemos PC, Serafim LS et al (2006) Recent advances in polyhydroxyalkanoate production by mixed aerobic cultures: from the substrate to the final product. Macromol Biosci 6:885–906. https://doi.org/10.1002/MABI.200600112
42. Stewart DE, Farmer FH (1984) Extraction, identification, and quantitation of phycobiliprotein pigments from phototrophic plankton. Limnol Oceanogr 29:392–397. https://doi.org/10.4319/LO.1984.29.2.0392
43. Xin J, Zhang Y, Dong J et al (2011) An experimental study on molecular weight of poly-3-hydroxybutyrate (PHB) accumulated in Methylosinus trichosporium IMV 3011. Afr J Biotechnol 10:7078–7087. https://doi.org/10.5897/AJB11.085
44. Song H, Xin J, Zhang Y et al (2010) Poly-3-hydroxybutyrate production from methanol by Methylosinus trichosporium IMV3011 in the nonsterilized fed-batch fermentation. African J Virol Res 5:1–8
45. Zhang Y, Xin J, Chen L, Xia C (2008) Biosynthesis of poly-3-hydroxybutyrate with a high molecular weight by methanotroph from methane and methanol. J Nat Gas Chem 17:103–109
46. Pieja AJ, Sundstrom ER, Criddle CS (2012) Cyclic , alternating methane and nitrogen limitation increases PHB production in a methanotrophic community. Bioresour Technol 107:385–392. https://doi.org/10.1016/j.biortech.2011.12.044
47. Zhang T, Zhou J, Wang X, Zhang Y (2016) ScienceDirect coupled effects of methane monooxygenase and nitrogen source on growth and poly- β -hydroxybutyrate (PHB) production of Methylosinus trichosporium OB3b. J Environ Sci 52:49–57. https://doi.org/10.1016/j.jes.2016.03.001
48. Shah NN, Hanna ML, Taylo RT (1995) Batch cultivation of Methylosinus trichosporium OB3b: V. Characterization of poly-β-hydroxybutyrate production under methane-dependent growth conditions. Biotechnol Bioeng 49(2):161–171
49. Rostkowski KH, Pfluger AR, Criddle CS (2013) Stoichiometry and kinetics of the PHB-producing Type II methanotrophs Methylosinus trichosporium OB3b and Methylocystis parvus OBBP. Bioresour Technol 132:71–77. https://doi.org/10.1016/j.biortech.2012.12.129
50. Bishoff D, AlSayed A, Eldyasti A (2021) Production of poly-hydroxy-butyrate using nitrogen removing methanotrophic mixed culture bioreactor. J Biosci Bioeng 132:351–358. https://doi.org/10.1016/j.jbiosc.2021.04.007
51. Pieja AJ, Sundstrom ER, Criddle CS (2011) Poly-3-hydroxybutyrate metabolism in the type II methanotroph Methylocystis parvus OBBP. Appl Environ Microbiol 77:6012–6019. https://doi.org/10.1128/AEM.00509-11
52. Bowman JP, Sayler GS (1994) Optimization and maintenance of soluble methane monooxygenase activity in Methylosinus trichosporium OB3b. Biodegradation:1. https://doi.org/10.1007/BF00695208
53. Choi DW, Kunz RC, Boyd ES et al (2003) The membrane-associated methane monooxygenase (pMMO) and pMMO-NADH: quinone oxidoreductase complex from Methylococcus capsulatus bath. J Bacteriol 185:5755–5764. https://doi.org/10.1128/JB.185.19.5755-5764.2003
54. Semrau JD, Dispirito AA, Yoon S (2010) Methanotrophs and copper. FEMS Microbiol Rev 34:496–531. https://doi.org/10.1111/j.1574-6976.2010.00212.x
55. Takeguchi M, Ohashi M (1999) Okura I (1999) Role of iron in particulate methane monooxygenase from Methylosinus trichosporium OB3b. Biometals 122(12):123–129. https://doi.org/10.1023/A:1009257826998
56. Zahn JA, Dispirito AA (1996) Membrane-associated methane monooxygenase from Methylococcus capsulatus (Bath). J Bacteriol 178:1018–1029. https://doi.org/10.1128/JB.178.4.1018-1029.1996

57. Murreil JC, Gilbert B, McDonald IR (2000) Molecular biology and regulation of methane monooxygenase. Arch Microbiol 173:325–332. https://doi.org/10.1007/S002030000158
58. Sihombing N, Elma M et al (2022) Garlic essential oil as an edible film antibacterial agent derived from Nagara sweet potato starch applied for packaging of Indonesian Traditional Food - Dodol. IOP Conf Ser Earth Environ Sci 999. https://doi.org/10.1088/1755-1315/999/1/012026
59. Ansari S, Fatma T (2016) Cyanobacterial polyhydroxybutyrate (PHB): screening, optimization and characterization. PLoS One 11:1–20. https://doi.org/10.1371/journal.pone.0158168
60. Ramezani M, Amoozegar MA, Ventosa A (2015) Screening and comparative assay of poly-hydroxyalkanoates produced by bacteria isolated from the Gavkhooni Wetland in Iran and evaluation of poly-β-hydroxybutyrate production by halotolerant bacterium Oceanimonas sp. GK1. Ann Microbiol 65:517–526. https://doi.org/10.1007/s13213-014-0887-y
61. Kovalcik A, Obruca S et al (2020) Enzymatic hydrolysis of poly(3-hydroxybutyrate-co-3-hydroxyvalerate) scaffolds. Materials 13(13):2992. https://doi.org/10.3390/ma13132992
62. Pradhan S, Dikshit PK, Moholkar VS (2018) Production, ultrasonic extraction, and characterization of poly (3-hydroxybutyrate) (PHB) using Bacillus megaterium and Cupriavidus necator. Polym Adv Technol 29:2392–2400. https://doi.org/10.1002/pat.4351
63. Mottin AC, Ayres E, Preto O, Horizonte B (2016) What changes in poly (3-hydroxybutyrate)(PHB) when processed as electrospun nanofibers or thermo-compression molded film? Mater Res 19:57–66
64. Shang L, Fei Q, Renewable N, Chang HN (2011) Thermal properties and biodegradability studies of poly (3-hydroxybutyrate- co -3-hydroxyvalerate). J Polym Environ 20:23
65. Helanto K, Matikainen L, Talj R, Rojas OJ (2019) Bio-based polymers for sustainable packaging and biobarriers: a critical review. BioResources 14:4902–4951. https://doi.org/10.15376/biores.14.2.Helanto
66. Bugnicourt E, Cinelli P, Lazzeri A, Alvarez V (2014) Polyhydroxyalkanoate (PHA): review of synthesis, characteristics, processing and potential applications in packaging. Express Polym Lett 8:791–808. https://doi.org/10.3144/expresspolymlett.2014.82
67. Kim YT, Min B, Kim KW (2014) General characteristics of packaging materials for food system. In: Innovations in food packaging. Academic Press, pp 13–35
68. Dadfar SMA, Alemzadeh I, Dadfar SMR, Vosoughi M (2011) Studies on the oxygen barrier and mechanical properties of low density polyethylene / organoclay nanocomposite films in the presence of ethylene vinyl acetate copolymer as a new type of compatibilizer. Mater Des 32:1806–1813. https://doi.org/10.1016/j.matdes.2010.12.028
69. Andersson T, Stålbom B, Wesslén B (2004) Degradation of polyethylene during extrusion. II. Degradation of low-density polyethylene, linear low-density polyethylene, and high-density polyethylene in film extrusion. J Appl Polym Sci 91:1525–1537. https://doi.org/10.1002/APP.13024
70. Emblem A (2012) Plastics properties for packaging materials. In: Packaging Technology. Woodhead Publishing, pp 287–309. https://doi.org/10.1533/9780857095701.2.287
71. Liu XJ, Zhang J, Hong PH, Li ZJ (2016) Microbial production and characterization of poly-3-hydroxybutyrate by Neptunomonas antarctica. PeerJ 4:e2291. https://doi.org/10.7717/PEERJ.2291
72. Zhu H, Wang Y, Zhang X et al (2007) Influence of molecular architecture and melt rheological characteristic on the optical properties of LDPE blown films. Polymer 48:5098–5106. https://doi.org/10.1016/j.polymer.2007.06.044